JOURNAL OF BACTERIOLOGY, June 1989, p. 3016–3024
0021-9193/89/063016-09$02.00/0

Vol. 171, No. 6

Organization of the *Haemophilus influenzae* Rd Genome

JOHN J. LEE, HAMILTON O. SMITH, AND ROSEMARY J. REDFIELD*

Department of Molecular Biology and Genetics, Johns Hopkins University School of Medicine, 725 North Wolfe Street, Baltimore, Maryland 21205

Received 14 November 1989/Accepted 8 March 1989

We present the first complete map of the *Haemophilus influenzae* genome, consisting of a detailed restriction map with a number of genetic loci. All of the *Apa*I, *Sma*I, and *Rsr*II restriction sites (total of 45 sites) were mapped by Southern blot hybridization analysis of fragments separated by pulsed-field gel electrophoresis. Cloned genes were placed on the restriction map by Southern hybridization, and antibiotic resistance loci were also located by transformation with purified restriction fragments. The attachment site of the HP1 prophage was mapped. In addition, the number, locations, and orientations of the six rRNA operons in the *H. influenzae* chromosome were determined. The positions of conserved restriction sites in these *rrn* operons confirm that the direction of transcription is 16S to 23S, as in most other bacteria. The widely used strain BC200 appears to contain an unexpected 45-kilobase duplication.

A major impediment to genetic analysis of the bacterium *Haemophilus influenzae* Rd has been the lack of a good genetic map. Although several partial genetic maps have been constructed by using cotransformation frequencies, they include only a small number of markers (about eight antibiotic resistances, an equal number of auxotrophic markers, and a few loci involved in recombination and DNA repair), and the maps are not without discrepancies (19, 34, 45). Progress in mapping has been impaired for two principal reasons. The first problem is the lack of genetic markers suitable for mapping. *H. influenzae* is a fastidious microorganism with many growth requirements; as a result, nutritional mutants cannot easily be isolated and characterized. The second problem is that conjugational and transductional mapping, so useful for *Escherichia coli* and *Salmonella typhimurium* genetics, has not been well developed for *H. influenzae*. spp. The natural transformation system of *H. influenzae* is efficient for mapping closely linked markers, but it is not suitable for large-scale mapping, and cotransformation frequencies depend on the fragment size of the DNA preparation used. Therefore, although a number of genes from *H. influenzae* have been identified and some have been cloned (see Table 3 for a partial list), it has not been possible to develop ideas about the overall genetic organization of this bacterium.

However, within the last few years the development of pulsed-field gel electrophoresis (42) has allowed very large DNA fragments to be separated and physical maps of several bacterial genomes to be constructed (4, 12, 44, 50). Here we present a detailed physical map of the *H. influenzae* Rd genome, constructed by Southern blot analysis of restriction fragments separated in pulsed-field gels.

MATERIALS AND METHODS

Strains and culture conditions. The *H. influenzae* strains used are listed in Table 1. Cells were grown in brain heart infusion broth (Difco Laboratories, Detroit, Mich.) supplemented with hemin (10 μg/ml) and NAD (2 μg/ml) (sBHI) with gentle shaking at 37°C or on sBHI plates containing 1.5% agar. Cells were made competent by the MIV procedure of Herriott et al. (20). Antibiotics were used in plates at the following concentrations (micrograms per milliliter): viomycin, 150; nalidixic acid, 3; novobiocin, 2.5; streptomycin, 250; kanamycin, 7; and spectinomycin, 20. Viomycin was obtained from Pfizer Inc. (New York, N.Y.); all other antibiotics were from Sigma Chemical Co. (St. Louis, Mo.).

DNA preparation and restriction digests. Preparation and restriction of high-molecular-weight genomic DNA embedded in agarose have been described by Lee and Smith (27). Conventional DNA preparation was done by the method of Maniatis et al. (31), omitting the lysozyme digestion. *Rsr*II was purchased from New England BioLabs (Beverly, Mass.) and used as recommended by the supplier.

Isolation and labeling of rRNA. Strain KW22 was grown in 250 ml of sBHI to an optical density at 650 nm of 0.3. Cells were pelleted at 5,000 × *g* for 15 min at 4°C and suspended in 5 ml of 30 mM Tris (pH 8.0)–20 mM EDTA–100 mM NaCl. Sodium dodecyl sulfate and proteinase K were added to concentrations of 1% and 100 μg/ml, respectively, and the suspension was incubated at 37°C for 1 h. After extraction with phenol and phenol-chloroform (1:1), samples were electrophoresed in a 1% low-melting-point agarose gel (SeaPlaque). The gel was stained with ethidium bromide, and the distinct 16S and 23S rRNA bands were excised. ^{32}P-labeled cDNAs to these RNAs were synthesized in agarose by a reverse transcriptase reaction (31).

Gel electrophoresis. Both OFAGE (orthogonal field alternation gel electrophoresis [8]) and CHEF (contour-clamped homogeneous field electrophoresis [10]) systems were used. OFAGE was preferred for Southern blot analysis because in our hands it gave sharper band resolution. Both systems used 1% agarose gels in 0.5× TBE (31) buffer at 0.5 to 5°C. OFAGE gels were run at 280 V for 12 h with pulse times ranging from 1 to 36 s, depending on the resolution range desired. CHEF gels were run at 195 V for 24 h with pulse times ranging from 6 to 80 s. Conventional gels (1.0% agarose) were run in TAE (31). Size standards for OFAGE and CHEF gels were lambda DNA concatemers generated in a standard ligation reaction (31). A 1-kilobase (kb) ladder and lambda DNA digested with *Hin*dIII (both from Bethesda Research Laboratories, Inc., Gaithersburg, Md.) were also used as size standards.

Most mapping was done by hybridizing gel-purified genomic restriction fragments, generated by one of the five restriction enzymes used, to sets of four Nytran filters

* Corresponding author.

TABLE 1. *H. influenzae* strains used

Strain	Serotype	Comment	Source or reference
KW20	Rd		H. Smith (laboratory strain)
KW22	Rd	Ery^r Str^r	H. Smith (laboratory strain)
MAP7[a]	Rd	Stv^r Str^r Vio^r Nal^r Spc^r Nov^r Kan^r	9
L-10	Rd	HP1 lysogen	48
BC200	Rd	Does not express defective prophage	2
TX100	a	Clinical isolate	E. Hansen[b]
DL42	b	Clinical isolate	18
TX101	c	Clinical isolate	E. Hansen[b]
TX102	d	Clinical isolate	E. Hansen[b]
CH205	f	Clinical isolate	E. Hansen[c]

[a] Ery^s derivative of MAP.
[b] Texas State Public Health Department, Austin.
[c] Childrens Memorial Hospital, Chicago, Ill.

(Schleicher & Schuell, Inc., Keene, N.H.). Each filter in a set was a Southern blot of a gel containing *Apa*I, *Eag*I, *Nae*I, and *Sma*I digests of KW22 DNA, run at a pulse time that would maximize resolution of a particular size range of fragments. The four pulse times used were as follows: OFAGE gel, 9-s cycle (best resolution of fragments, >150 kb); OFAGE gel, 3-s cycle (50 to 150 kb); OFAGE gel, 1-s cycle (5 to 50kb); and conventional gel, 1% agarose (<10 kb).

Southern hybridization. DNA was transferred onto Nytran membranes and then baked, prehybridized, hybridized, washed, exposed, and eluted under conditions recommended by the supplier. DNAs were labeled by the random-oligonucleotide priming method (13). Most genomic DNA fragments were labeled directly in agarose, but some small fragments were first concentrated by using GeneClean (Bio101).

Transformational mapping. To map antibiotic resistance genes, bands containing the restriction fragments of strain MAP7 were excised from a low-melting-point agarose gel under long-wave UV illumination. The gel slices were melted at 65°C, and 2 μl was added to 0.2 ml of competent KW20 cells. After 30 min of incubation, 2 ml of sBHI was added, and the cells were grown for 1 h before dilution and plating with and without the antibiotic to be mapped.

RESULTS

Lee and Smith (27) demonstrated that the four restriction enzymes *Apa*I (5′-GGGCCC), *Eag*I (5′-CGGCCG), *Nae*I (5′-GCCGGC), and *Sma*I (5′-CCCGGG) cut the DNA of *H. influenzae* Rd KW22 into restriction fragments suitable for mapping. Subsequently, we found that *Rsr*II (5′-CGG^A_TCCG) cuts KW22 DNA at only four sites. We have now determined, by using both OFAGE and CHEF separation systems, the sizes of all restriction fragments generated by these enzymes; our current best estimates are given in Table 2. Except for several new small *Nae*I fragments, only minor size changes have been made from the previously published values (27). Reconstruction experiments with *Hin*dIII-digested lambda DNA indicated that in our gels, we could reliably detect a band containing 0.5 ng of a 500-base-pair (bp) fragment (equivalent to a single-copy band from 2 μg of *H. influenzae* genomic DNA). Since we ran 5 μg of DNA in our conventional gels, we are fairly confident that we have not overlooked any fragments larger than 500 bp. The fragments listed in Table 2 sum to genome sizes of between 1,885 and 1,907 kb; for mapping, we have assumed a genome size of 1,900 kb.

TABLE 2. Sizes of restriction fragments of *H. influenzae* Rd KW22 DNA

Fragment	Fragment size (kb)				
	*Apa*I	*Eag*I	*Nae*I	*Sma*I	*Rsr*II
A	305	345	295	380	630
B	290	255	195	260	610
C	240	240	175	230	420
D	215	125	140	220	230
E	120	105	135	190	
F	100	95	110	160	
G	90	75	105	135	
H	83	65	100	90	
I	78	60	100	75	
J	70	58	80	45	
K	54	57	70	34	
L	47	54	65	24	
M	39	52	55	21	
N	38	41	45	13	
O	32	40	31	9.5	
P	32	39	28	6.2	
Q	21	34	23		
R	18	26	20		
S	2.9	25	19		
T	1.75[a]	23	17		
U	1.5[a]	20	16.5		
V		16.5	15		
W		13.5	14		
X		13	10.5		
Y		10	8.0		
Z		3.35[a]	6.0		
AA		3.1[a]	5.3		
BB		0.6	5.3		
CC			3.3		
DD			3.2		
EE			3.1		
FF			2.5		
GG			2.3		
HH			0.77		
II			0.74		
JJ			0.64		
Total	1,885	1,907	1,905	1,893	1,890

[a] The *Apa*I-T and -U and *Eag*I-Z and -AA bands are actually each three fragments of identical sizes derived from the six rRNA operons (see text). This has been taken into account in calculating the totals.

We compared the *Apa*I and *Sma*I patterns of KW22 with those of the other *H. influenzae* strains listed in Table 1. Figure 1 shows the *Sma*I patterns of five clinical isolates of different serotypes. The clinical serotype d isolate TX102 (lane 4) was identical to KW22 (27); the patterns of the other serotypes (lanes 1, 2, 3, and 5) differed from that of Rd and from each other at most positions. Strains KW20 and MAP7 (not shown) had patterns identical to that of KW22 for all enzymes used; we have occasionally used them in place of KW22 for Southern blots and probes. Strains L-10 and BC200 are discussed below.

Characterization of the *H. influenzae* rRNA operon repeats. Lee and Smith (27) reported that the *Eag*I 3.35- and 3.1-kb bands (Z and AA) each contained at least two comigrating DNA fragments. Inspection of *Apa*I and *Sac*II digests showed that these enzymes also produced pairs of multiple-copy bands differing in size by 0.25 kb (*Apa*I bands T and U of 1.75 and 1.5 kb and unnamed *Sac*II bands of 3.8 and 3.55

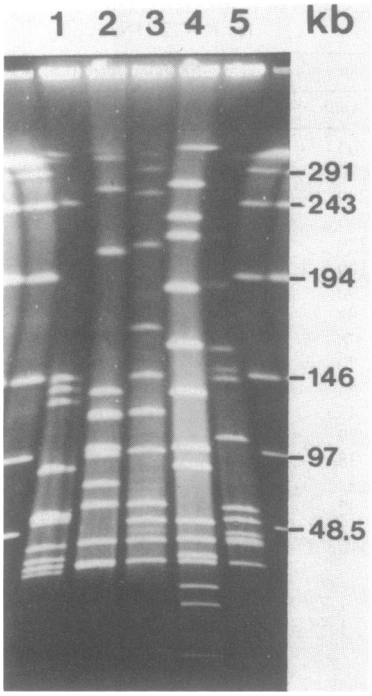

FIG. 1. *Sma*I digestion patterns of examples of different *H. influenzae* serotypes. OFAGE gel was run with a 9-s pulse time. Lanes: 1, TX100 (serotype a); 2, DL42 (serotype b); 3, TX101 (serotype c); 4, TX102 (serotype d); 5, CH205 (serotype f). The flanking lanes contain lambda concatemers.

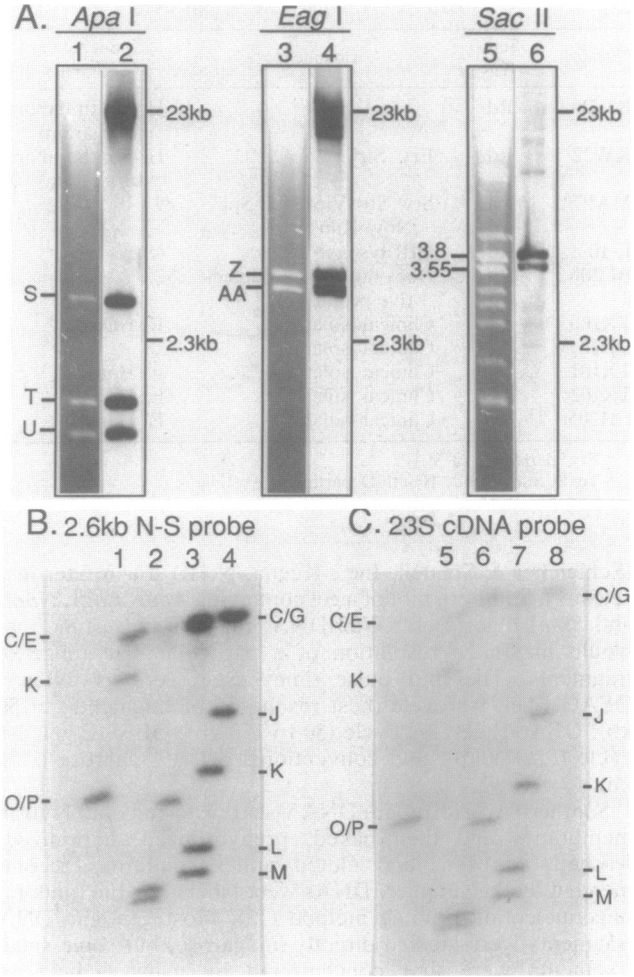

FIG. 2. (A) Small multiple-copy fragments containing rRNA sequences. Lanes: 1, 3, and 5, ethidium-stained gel; 2, 4, and 6, Southern blot hybridized with ^{32}P-labeled cDNA to 23S rRNA; 1 and 2, *Apa*I; 3 and 4, *Eag*I; 5 and 6, *Sac*II. (B and C) Demonstration that 23S cDNA and a subfragment of the repeated element hybridize to the same fragments. (B) 2.6-kb *Nae*I-*Sma*I genomic subfragment probe (see Fig. 3); (C) 23S cDNA probe. Lanes: 1, *Apa*I; 2, *Eag*I; 3, *Nae*I; 4, *Sma*I. The OFAGE gels used in panels B and C were not identical; each was run for approximately 12 h with a 3-s pulse. *Apa*I bands detected by the probes are labeled on the left; *Sma*I bands are labeled on the right.

kb; Fig. 2A, lanes 1, 3, and 5). Densitometer scanning indicated that these bands each contained three or possibly four times as much DNA as expected for single-copy fragments. This can be seen by comparing the intensities of the *Apa*I bands T and U in Fig. 2A with that of the single-copy *Apa*I band S above them. We therefore thought that the DNA in these bands might come from within two repetitive elements in the genome. The hybridizations described below showed that these bands were derived from the six copies of the rRNA operon present in *H. influenzae*.

Southern analysis using the filter sets described in Materials and Methods initially demonstrated that the *Apa*I and *Eag*I multiple-copy fragments (*Apa*I-T and -U and *Eag*I-Z and -AA) all had sequences in common. When each fragment was used as a probe, it hybridized strongly to all four bands. Three further observations led us to preliminary maps of the repeated sequences in these bands. (i) *Apa*I-T and -U probes each hybridized with equal intensity to both *Apa*I-T and -U. Similarly, the *Eag*I-Z and -AA probes each hybridized equally to both *Eag*I-Z and -AA. This suggested that the pairs of fragments were almost entirely homologous. (ii) The *Apa*I-T and -U probes hybridized to many different bands in *Nae*I and *Sma*I digests but only to the multicopy bands in *Apa*I and *Eag*I digests. This suggested that the *Apa*I fragments T and U were internal subfragments of the *Eag*I fragments Z and AA. (iii) All four of the multicopy probes gave the same pattern of hybridization to *Nae*I and *Sma*I digests. In the *Sma*I digest, each hybridized strongly to the C, G, J, K, L, and M bands and weakly to the A, H, I, N, and O bands. Unlike the *Apa*I multicopy probes, which hybridized only to the multicopy bands in *Eag*I digests, the *Eag*I-Z and -AA probes hybridized weakly to five or six additional, single-copy bands in *Apa*I digests (C, E, K, O/P, and S). These observations suggested that the *Apa*I fragments T and U (1.75 and 1.5 kb) and the *Eag*I fragments Z and AA (3.35 and 3.1 kb) might be derived from copies of a single type of repetitive element that was present in two size classes, one 0.25 kb bigger than the other. The elements would contain two *Apa*I sites internal to two *Eag*I sites, and the 0.25-kb length polymorphism would be internal to the *Apa*I sites. Southern blot analysis of the small fragments produced by double digestions confirmed this hypothesis, giving the more detailed map shown in Fig. 3.

The concentration of G+C-rich restriction sites in these repeated elements relative to the *H. influenzae* genome, which is only 37% G+C (40), suggested that these elements might be rRNA operons. This was confirmed by probing with an *E. coli rrnB* plasmid (6) and with ^{32}P-labeled cDNAs to 16S and 23S rRNAs isolated from *H. influenzae*. The *E. coli rrnB* probe hybridized weakly to all bands we had

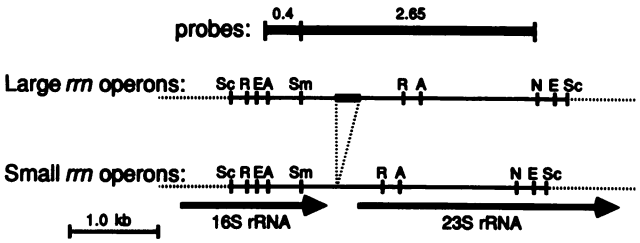

FIG. 3. Restriction maps of two size classes of rRNA operons. Abbreviations for restriction sites: R, *Eco*RI; Sc, *Sac*II; A, *Apa*I; E, *Eag*I; N, *Nae*I; Sm, *Sma*I. The 250-bp length polymorphism is indicated by a thick bar. It has been mapped only to within the 0.9/1.15-kb *Eco*RI-*Sma*I fragments.

identified as containing the repeated elements. Examples of probing with 23S cDNA and with the 2.65-kb *Nae*I-*Sma*I subfragment of the repeated element (gel purified from total genomic DNA) are shown in Fig. 2. The 23S cDNA hybridized strongly to the *Apa*I, *Eag*I, and *Sac*II multicopy bands (Fig. 2A, lanes 2, 4, and 6), to *Apa*I fragments C, E, K, O/P, and S, and to *Sma*I fragments C, G, J, K, L, and M (Fig. 2B). (Only some of these bands are resolved in Fig. 2.) These were the same fragments detected by the 2.65-kb genomic subfragment (Fig. 2B). The 16S cDNA probe similarly hybridized to the *Apa*I and *Eag*I multicopy bands, to *Apa*I fragments A, E, H, I, and L, weakly to *Sma*I fragments C, G, J, K, L, and M, and strongly to *Sma*I fragments A, H, I, K, N, and O. These are the same fragments detected by the 0.4-kb *Apa*I-*Sma*I subfragment of the repeated element. This analysis also indicated that there were six copies of the rRNA operons in the genome. We have mapped these loci (Fig. 4) and named them *rrnA*, *rrnB*, etc., in clockwise order around the genome.

We also examined the rDNA fragments of the clinical *H. influenzae* isolates by probing with the 16S and 23S cDNA probes from KW22 (data not shown). When digested with *Eag*I and *Sac*II, all isolates gave small pairs of intensely hybridizing bands separated by 250 bp. The bands of serotypes a, f, and d were of the same size as those of KW22; the bands of serotypes b and c were about 200 bp larger. When cut with *Apa*I, only serotypes b and d showed pairs of small bands (1.75 and 1.5 kb). The other serotypes therefore appear to lack at least one of the *Apa*I sites present in Rd.

Mapping with *Rsr*II. *Rsr*II was the only restriction enzyme we found that cut the genome into a workable number of fragments (≤35) but did not cut in the *rrn* operons. Because *Apa*I, *Eag*I, *Nae*I, and *Sma*I cut in the ribosomal repeats, analysis using only these enzymes would have led to restriction maps of six segments bounded by the ribosomal operons but could not have established the relationships between the segments. *Rsr*II therefore provided an essential tool for constructing a restriction map of the genome. In Fig. 4, we present complete maps of the *Rsr*II, *Apa*I, and *Sma*I sites of strain KW22; because some of the *Eag*I and *Nae*I fragments were not well resolved in Southern blots, we have not yet completed their maps. We present below only sufficient evidence to establish the order of the fragments on the map and do not in general discuss the corroborating evidence from reciprocal hybridizations, double digests, or consider-

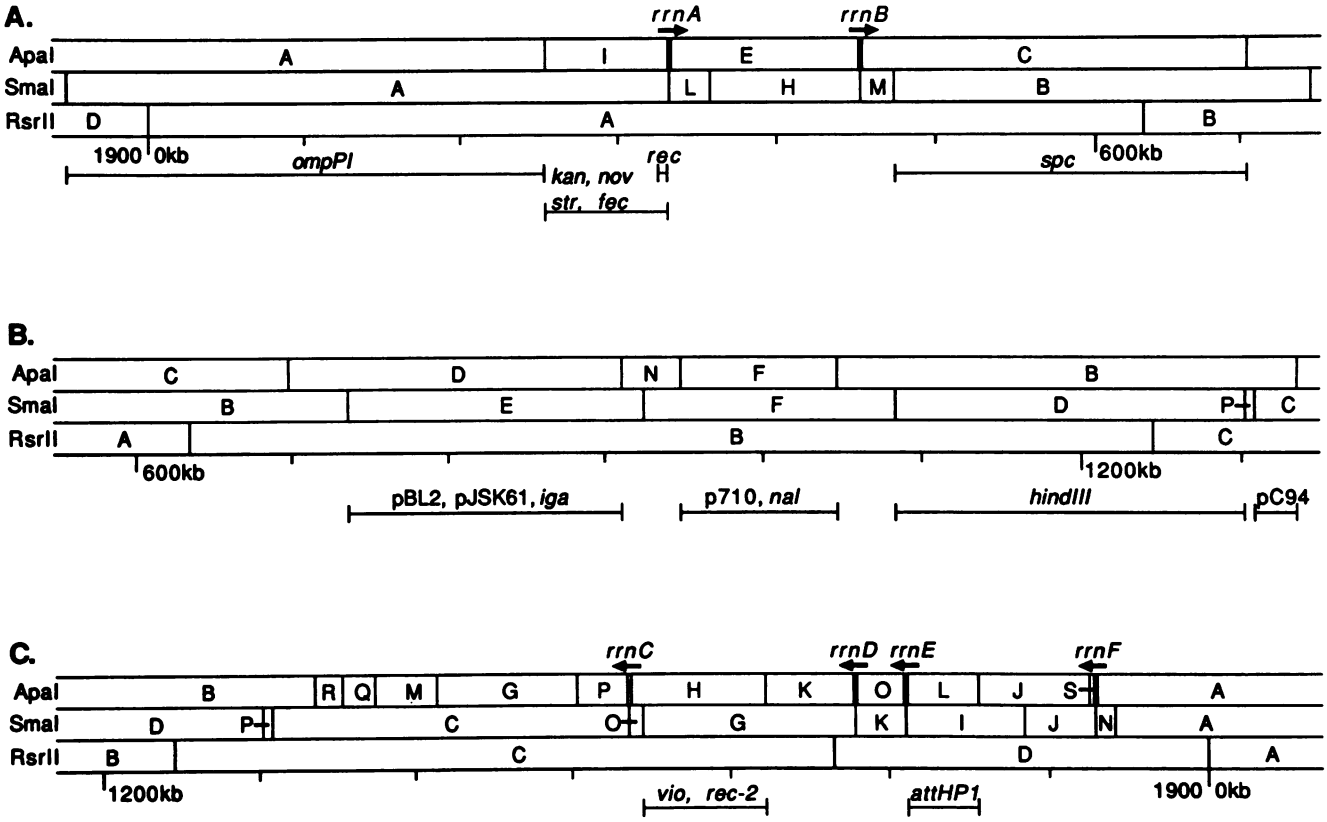

FIG. 4. Restriction maps of the *H. influenzae* Rd genome. (A) *Rsr*II fragment A; (B) *Rsr*II fragment B; (C) *Rsr*II fragments C and D. Locations of rRNA operons are indicated above the maps; those of other loci are shown below the maps.

ations of fragment sizes. When fitting the fragments onto the map in Fig. 4, we have allowed for errors of up to 5% in our fragment size estimations; therefore, similar uncertainties may be associated with the positions of the restriction sites that flank each fragment.

Several factors had to be taken into account when mapping very large restriction fragments. Because the largest fragments suffered the most from random breakage (compare the intensities of the large and small fragments in Fig. 1), the relative intensities of hybridization of large and small fragments did not always reflect the relative length of homology with the probe. Specifically, a probe that hybridized more strongly to the smaller of two fragments did not necessarily have more homology to that fragment. Another consequence of random degradation (and possibly of gradual release of DNA fragments trapped in the wells) was that gel-purified genomic fragment probes usually contained small amounts of randomly broken DNA from the rest of the chromosome and therefore hybridized faintly to all fragments. Although this background hybridization prevented us from detecting any very short overlaps, it did allow us to make more reliable fragment identifications in Southern blots by examining overexposed films. We anticipated that the presence of the *rrn* operons identified above on fragments used as probes could confound our Southern analysis, so we probed a filter of an *Rsr*II digest with the 3.8-kb *Sac*II fragment (see Fig. 2) to determine how they were distributed among the *Rsr*II fragments. We found strongest hybridization to *Rsr*II-D, moderate hybridization to *Rsr*II-A, weak hybridization to *Rsr*II-C, and no hybridization to *Rsr*II-B. We took this homology into account when probing *Rsr*II digests with fragments known to contain rRNA sequences.

The first step in mapping was to assign the *Apa*I and *Sma*I fragments to specific *Rsr*II fragments by hybridizing them to filters of *Rsr*II-cut KW22 DNA. Fragments hybridizing to two *Rsr*II fragments allowed us to link the *Rsr*II fragments into a simple circular map, onto which the remaining *Apa*I and *Sma*I fragments could be mapped. *Apa*I-C hybridized to *Rsr*II-A and -B, *Apa*I-B hybridized to *Rsr*II-B and -C, *Apa*I-K hybridized to *Rsr*II-C and -D, and *Apa*I-A hybridized to *Rsr*II-A and -D. (*Apa*I-K also hybridized weakly to *Rsr*II-A; we think this was because it is a small fragment containing 16S rDNA.) Double digests with *Apa*I plus *Rsr*II confirmed that these *Apa*I fragments each contained an *Rsr*II site. Similarly, *Sma*I-B, -D, and -A hybridized to *Rsr*II fragments A and B, B and C, and D and A, respectively (*Sma*I-G hybridized strongly to *Rsr*II-C and weakly to fragments D and A); however, *Rsr*II-*Sma*I double digests showed degradation of large fragments and, although consistent with the map order above, were not informative. The *Apa*I and *Sma*I fragments thus linked the *Rsr*II fragments into a circular map with the order A-B-C-D. We have numbered the map positions in kilobases from 0 at the start of *Rsr*II-A to 1,900 at the end of *Rsr*II-D.

(i) *Apa*I and *Sma*I fragments in *Rsr*II-A. *Rsr*II-A was strongly hybridized to by *Apa*I fragments A, C, E, and I and by *Sma*I fragments A, B, H, L, and M (Fig. 4A). *Apa*I-A and *Sma*I-A also hybridized to *Rsr*II-D, and *Apa*I-A was cut by *Rsr*II into fragments of 235 and 70 kb. We placed the 235-kb subfragment in *Rsr*II-A because it hybridized more strongly to *Rsr*II-A than to *Rsr*II-D. Similarly, because *Apa*I-C spanned *Rsr*II-A and -B, was cut into 175- and 65-kb fragments, and hybridized more strongly to *Rsr*II-A than to *Rsr*II-B, we placed its 175-kb subfragment in *Rsr*II-A. We placed *Sma*I-B with *Apa*I-C because they hybridized to each other and to *Rsr*II-B. We used hybridizations of *Apa*I and *Sma*I fragments to each other in the filter sets described in Materials and Methods to map fragments within *Rsr*II-A. *Sma*I-A hybridized to *Apa*I-A and -I, and *Apa*I-I hybridized only to *Sma*I-A. *Apa*I-E hybridized to *Sma*I-L and -H, and *Apa*I-C hybridized to *Sma*I-B and -M. Because *Sma*I-L contains 23S rRNA sequences and *Sma*I-H contains 16S rRNA sequences, we placed them adjacent to *Sma*I-A (16S) and *Sma*I-M (23S), respectively, where they would contribute to complete *rrn* operons.

(ii) *Apa*I and *Sma*I fragments in *Rsr*II-B. *Rsr*II-B was hybridized to by *Apa*I fragments B, C, D, F, and M/N and by *Sma*I fragments B, D, E, and F (Fig. 4B). Because *Apa*I-M and -N could not be resolved in preparative gels, they were used together as a mixed probe. However, they were often well enough resolved in Southern blots that we have identified the bands in *Rsr*II-B as *Apa*I-N and that in *Rsr*II-C as *Apa*I-M. *Apa*I-B and *Sma*I-D also hybridized to *Rsr*II-C and to each other, and *Apa*I-B was cut by *Rsr*II into fragments of 200 and 80 kb. *Apa*I-D hybridized to *Sma*I-B and -E, *Sma*I-E hybridized to *Apa*I-D and -N, and *Sma*I-F hybridized to *Apa*I-N, -F, and -B.

(iii) *Apa*I and *Sma*I fragments in *Rsr*II-C. *Rsr*II-C was hybridized to by *Apa*I fragments B, G, H, K, N, O/P, Q, and R and by *Sma*I fragments C, D, G, O, and P (Fig. 4C). *Apa*I-O and -P comigrated, so we have designated the 31-kb *Apa*I fragment in *Rsr*II-C as P and the one in *Rsr*II-D as O. *Apa*I-K and *Sma*I-G hybridized strongly to each other and weakly to *Rsr*II-D, so we placed them at the right end of *Rsr*II-C. *Sma*I-O hybridized strongly to *Apa*I-H and weakly to all 16S rDNA fragments (including *Rsr*II-A and -D). At the left end of *Rsr*II-C, *Apa*I-B hybridized to *Sma*I fragments F, D, P, and C, and *Apa*I fragments R, Q, and G hybridized only to *Sma*I-C. *Sma*I-P hybridized only to *Apa*I-B. An *Apa*I-M/N probe hybridized to *Sma*I-C and to *Sma*I-E and -F (both in *Rsr*II-B), whereas an *Apa*I-O/P probe hybridized strongly to *Sma*I-C and to *Sma*I-K (in *Rsr*II-D) and weakly to fragments containing 16S or 23S rDNA (more strongly to those with 23S). Because *Apa*I-P was the only *Apa*I fragment in *Rsr*II-C that contained 23S rRNA sequences, we placed it next to the 16S-containing fragments *Apa*I-H and *Sma*I-O. *Apa*I fragments R, Q, M, and G were ordered by hybridization with *Eag*I and *Nae*I probes. *Nae*I-J hybridized to *Sma*I-C and -P and to *Apa*I fragments M/N, Q, R, and (weakly) B. *Nae*I-D hybridized to *Sma*I-C and to *Apa*I fragments G, M/N, and O/P. We placed *Apa*I-Q to the right of *Apa*I-R because *Eag*I-H hybridized strongly to *Apa*I fragments M/N and Q but only weakly to fragment R.

(iv) *Apa*I and *Sma*I fragments in *Rsr*II-D. *Rsr*II-D was hybridized to by *Apa*I fragments A, J, K, L, and O/P and by *Sma*I fragments A, G, I, J, K, and N (Fig. 4C). At the right end of *Rsr*II-D, *Apa*I-A hybridized to *Sma*I-N and -A, and *Sma*I-N hybridized to *Apa*I-A and to other bands containing 16S rDNA. *Sma*I-K and *Apa*I-O/P hybridized strongly to each other and weakly to all other rDNA-containing fragments (*Apa*I-O/P also hybridized strongly to *Sma*I-C). *Apa*I-J hybridized to *Sma*I-I and -J, and *Sma*I-I hybridized to *Apa*I-L and -J and to the other bands containing 16S rDNA. *Sma*I-J hybridized to *Apa*I-J and 23S-containing bands, and *Apa*I-L hybridized to *Sma*I-I and 16S-containing bands. The order of *Sma*I fragments (G-K-I-J-N rather than G-I-J-K-N) was determined by analysis of *Sma*I partial digests; a 55-kb partial-digestion fragment hybridizing to *Sma*I-K was diagnostic for this orientation. We were unable to map *Apa*I-S by Southern analysis; it is only 2.9 kb long and hybridized more

TABLE 3. Placing of genetic markers on the restriction map

Locus (plasmid)	Fragment				Source or reference
	*Apa*I	*Eag*I	*Nae*I	*Sma*I	
Mapped by hybridization[a]					
(pBL2)	D	B	F	E	E. R. Moxon
(pJSK61)[b]	D	J/K[c]	F	E	E. R. Moxon
(pC94)[b]	B	N/O/P[c]	J	C	E. R. Moxon
(p710)[b]	F	I	C	F	E. R. Moxon
Pl (pRSM150)	A	A	A	A	36
rec-2 (pDM62)	H	G	D/E[c]	G	32
strA (pKLT1)	I	T	A	A	33
nov-1 (pNov1)	I	T	A	A	43
iga (pFG26)	D	B	F	E	17
rec (pGBH1)	I	S/T[c]	A	A	G. Barcak
fec (pGBFR1)	I	T	A	A	G. Barcak
hindIIIRM	B	C	B	D	30
Mapped by transformation[d]					
Str[r]	I			A	MAP7
Kan[r]	I			A	MAP7
Nov[r]	I			A	MAP7
Spc[r]	C			B	MAP7
Nal[r]	F			F	MAP7
Vio[r]	H			G	MAP7

[a] Fragments are those to which the probe hybridized.
[b] Locus involved in virulence expression, cloned from serotype b strains (E. R. Moxon, personal communication). All other clones are from serotype d.
[c] Fragments could not be resolved in Southern blots.
[d] Fragments are those that efficiently transformed KW20 to antibiotic resistance.

or less equally to all bands containing 23S rDNA. We have placed it to the right of *Apa*I-J, which is on the 23S side of the *Apa*I sites in *rrnF* but does not appear to contain the expected 23S sequences.

Placement of genetic markers on the restriction map. We used Southern hybridization to the filter sets to place a number of cloned genes on the restriction map. The probes used and the fragments they hybridized to are listed in Table 3. The map positions indicated by this analysis are shown below the restriction maps in Fig. 4. We have placed the cloned *rec* gene (1a) at *rrnA* because it contains 16S rRNA sequences and the corresponding *Eco*RI and *Sac*II restriction sites (Fig. 3).

We also mapped six antibiotic resistance genes by transformation with gel-purified restriction fragments of the multiple-antibiotic-resistant strain MAP7 (an erythromycin-sensitive derivative of MAP [9]). The antibiotic-sensitive strain KW20 was transformed with each of the *Sma*I fragments of MAP7. For each marker, a single fragment gave a high frequency of antibiotic-resistant transformants. These *Sma*I fragments all contained *Apa*I sites, so the positions of the resistance genes were narrowed by transformation of KW20 with the corresponding *Apa*I fragments of MAP7. The fragments carrying these resistance genes are listed in Table 3, and the resulting map positions are shown below the restriction maps in Fig. 4.

The attachment site for the 32-kb *H. influenzae* bacteriophage HP1 (15) was also mapped. The *Apa*I and *Sma*I restriction patterns of the HP1 lysogen L-10 were compared with those of KW20 (not lysogenic for HP1). The *Apa*I-L (47-kb) and *Sma*I-I (75-kb) fragments were missing in L-10 DNA, and in both digests there were single new bands (*Apa*I [77 kb] and *Sma*I [105 kb]) that hybridized to an HP1 probe.

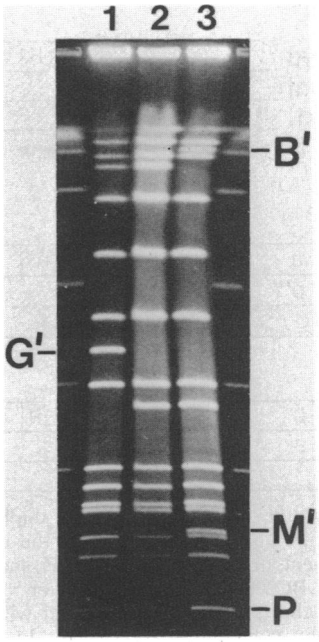

FIG. 5. *Sma*I digestion patterns of strains L-10 (lane 1), KW20 (lane 2), and BC200 (lane 3). The flanking lanes contain lambda concatemers. The OFAGE gel was run with an 8-s pulse.

The *Sma*I patterns of L-10 and KW20 are shown in lanes 1 and 2 of Fig. 5; the novel 105-kb L-10 band is labeled G'.

Strain BC200 is an Rd derivative that has been widely used because it does not express the defective prophage seen in other Rd strains (3). We examined its *Apa*I, *Eag*I, and *Sma*I patterns, expecting to be able to map a site of prophage excision by identifying fragments whose sizes had decreased. However, we found that the BC200 genome was larger rather than smaller than that of other Rd strains. Lane 3 of Fig. 5 shows a *Sma*I digest of BC200 DNA. Comparison with a digest of KW20 DNA (lane 2) shows that fragment D (220 kb) is missing, fragment P (6.2 kb) is of double intensity, and there are two new fragments of 245 kb (B', between B and C) and 14 kb (M', just above N). In *Rsr*II digests, fragment C was increased from 420 to 465 kb; in *Apa*I digests, fragment B (290 kb) was missing, fragment R was of double intensity, and there were two new fragments of 240 (C') and 75 (I') kb (not shown).

Southern blot analysis (not shown) suggested that BC200 carries the inverted duplication shown in Fig. 6. The double-intensity *Sma*I-P and *Apa*I-R bands of BC200 hybridized only to *Sma*I-P and *Apa*I-R sequences, respectively, in both BC200 and KW22 DNAs, which suggested that the 43-kb DNA segment containing these fragments was duplicated in BC200. In *Sma*I digests, the BC200 B' fragment hybridized to the B' and C fragments of BC200 and to the C and D fragments of KW22; M' hybridized only to itself in BC200 digests and only to fragment D in KW22 digests. The KW22 *Apa*I-B fragment hybridized to BC200 *Apa*I bands of 240 (C or C') and 75 (I or I') kb and to BC200 *Sma*I fragments B' and N' (as well as faintly to the expected *Sma*I fragments C, F, and P). The new BC200 *Apa*I fragments (C' and I') could not be separated from fragments C and I, so their hybridization patterns were more complex; however, all of the hybridization results were consistent with the inverted duplication shown in Fig. 6.

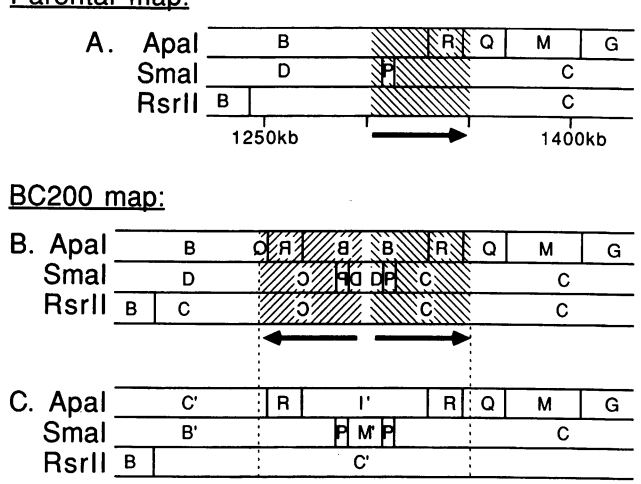

FIG. 6. Map of the postulated inverted duplication in strain BC200. (A) Structure of typical Rd strains in the 1,250- to 1,400-kb region. The segment duplicated in BC200 is shaded. (B and C) Identical maps of BC200 over the same region. In panel B, fragments altered by the duplication are labeled with their previous designations; duplicated regions are shaded. In panel C, altered fragments are labeled as the new fragments they have become.

DISCUSSION

The restriction map of *H. influenzae* Rd presented here is one of the few complete bacterial restriction maps constructed entirely by physical methods (4, 26) and the first to be determined entirely by Southern blot analysis of fragments separated by pulsed-field gels. We were not able to use cloned genes and genetic markers for construction of the map, as was done for the large-fragment map of *E. coli* K-12 (44). Rather, genes and other markers available for *H. influenzae* were located after the physical restriction map had been established.

The results presented here, although sufficient to justify the map, are only a portion of the total evidence on which the map is based. All of the *Apa*I, *Eag*I, *Nae*I, *Rsr*II, and *Sma*I fragments have been probed with every *Apa*I and *Sma*I fragment and with many *Eag*I and *Nae*I fragments. *Apa*I-*Sma*I double digests have also been probed with a number of fragments. All of this analysis is consistent with the map in Fig. 4. Furthermore, although the relative positions of fragments were usually determined without reference to the placement of 16S and 23S rRNA sequences, they yielded a map with complete *rrn* operons. We have estimated fragment sizes with two different pulsed-field electrophoresis systems, and the resulting fragments fit into the map to a tolerance of within 5%.

An independent clinically isolated serotype d strain, TX102, gave a restriction pattern indistinguishable from that of KW22 and other descendants of the original Rd strain of Alexander and Leidy (1). This is consistent with the finding by Musser et al. that type d *H. influenzae* strains form an evolutionarily tight group (37). The restriction patterns of different serotypes are very distinct and suggest that similar comparisons might provide a useful additional method of strain characterization. The patterns may be more diverse than we have seen. We have examined only a single isolate of types a, b, c, and f and no isolates of serotype e or of any nontypable strains. Furthermore, strains of types a and b fall into several distinct evolutionary groups whose *cap* loci have related but distinct restriction patterns (37), and these groups may have genomic restriction maps as different as those of different serotypes. The different patterns of the different serotypes need not mean that their genomes are grossly dissimilar. Rather, many of the differences may be due to restriction site polymorphisms, small insertions and deletions, and chromosome rearrangements, as are seen between *E. coli* and *S. typhimurium* (39).

Before this study, nothing was known about the genes for rRNA in *H. influenzae*. We have identified and mapped six rRNA operons and believe that this is the full complement because (i) our mapping would have detected the *Apa*I and *Sma*I sites of any other isolated copies and (ii) any other tandem copies would have given rise to short telltale restriction fragments. Six copies is about the middle of the range seen in bacteria: *Bacillus subtilis* has ten (23), *E. coli* and *S. typhimurium* each have seven (11, 28), *Streptomyces coelicolor* has six (5), *Caulobacter crescentus* (14), *Anacystis nidulans* (47), and *Mycoplasma capricolum* (16) each have two, and *Halobacterium halobium* has only one (21). The number of copies of the rRNA operons does not correlate well with genome size (for example, the ratio in *H. influenzae* is more than twice that in *E. coli*) but has been suggested to be directly related to generation time (14). In rich medium, *H. influenzae* has a generation time of 29 min, compared with 20 min for *E. coli*.

The chromosomal locations of rRNA operons have been mapped in only a few bacterial species (*B. subtilis* [23], *E. coli* [11], and *S. typhimurium* [28]). Comparison of the restriction sites in the *H. influenzae* 16S region (Fig. 3) with those seen to be highly conserved within other eubacterial 16S rRNA sequences (5′-*Sac*II, *Eco*RI, *Apa*I, *Sma*I-3′ [22]) shows that the *H. influenzae* rRNA operons, like those of most other eubacteria, are transcribed from 16S to 23S. The same comparison predicts that the 16S gene should begin about 520 bp upstream of the left *Sac*II site and end 160 bp beyond the *Sma*I site. Similarly, comparison with the *E. coli rrnB* map (5) suggests that the 23S sequences will extend about 900 bp beyond the right *Sac*II site.

The two size classes of *rrn* operons may differ in the presence of tRNA genes in the spacers between 16S and 23S sequences, as has been seen in other bacterial rRNA operons. In both *E. coli* (35) and *S. typhimurium* (28), four *rrn* loci contain a single $tRNA^{Glu}$ gene, and the other three contain genes for $tRNA^{Ile}$ and $tRNA^{Ala}$. *B. subtilis*, like *H. influenzae*, has two size classes of rRNA operons, with spacers differing by about 0.2 kb. There are no tRNA genes in the smaller spacer and $tRNA^{Ile}$ and $tRNA^{Ala}$ genes in at least one of the large spacers (29). $tRNA^{Ile}$ and $tRNA^{Ala}$ also are found in the spacer of *C. crescentus* (14) and in the chloroplast rRNA operon spacers of *Zea mays*, *Euglena gracilis*, and *Nicotiana tabacum* (24, 25, 46). We expect that they will also be found in the large copies of the *H. influenzae* rRNA operons.

In *E. coli* and *B. subtilis*, transcription of the ribosomal operons is directly away from the origin of chromosomal replication (11, 23); this is thought to minimize collisions between DNA and RNA polymerases (7). The six *H. influenzae* operons are all transcribed away from a common region (Fig. 7), so the origin of replication may be found between *rrnF* and *rrnA*.

Our experience with restriction sites in the rRNA operons should provide a caution to others attempting to develop restriction maps of bacterial genomes. It will be essential to use at least one restriction enzyme that does not cut in the *rrn* operons; otherwise, only the intervals between these

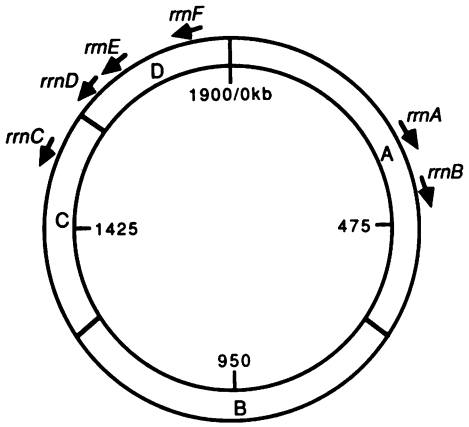

FIG. 7. Locations and orientations of the rRNA operons around the *H. influenzae* chromosome. *Rsr*II fragments are indicated.

repeats can be mapped. This will be a problem particularly when mapping small A+T-rich genomes, when *Apa*I, *Eag*I, *Nae*I, *Sac*II, and *Sma*I might otherwise be the enzymes of choice. Similar problems may arise whenever a genome contains other repeated elements, especially any whose base composition differs strongly from that of the rest of the genome.

Our hybridizations did not detect any repeated elements other than the *rrn* operons, but the sensitivity was limited because the restriction fragments isolated from genomic DNA contained small amounts of total DNA. We might not have detected multiple copies of short sequences such as insertion elements, especially if they were present only in the large fragments.

This map is the first complete map of the *H. influenzae* genome; like the maps for other bacteria, it is circular (Fig. 7). How does our placement of genetic markers compare with the previously reported partial maps of *H. influenzae* Rd (19, 34, 41, 45)? *str*, *nov*, and *kan* are closely linked genetically and in our map (all on *Sma*I-A and *Apa*I-I), and the gene order (*str*, *nov*, *kan*)-*spc*-*nal*-*vio* is also in agreement with published maps. However, we place the HP1 attachment site between *vio* and (*str*, *nov*, *kan*) rather than between *nal* and *vio* (45). Michalka and Goodgal estimated the physical distances separating loci by the dependence of cotransformation frequencies on the size of sheared preparations of transforming DNA (34). By this technique, *kan* and *nal* were estimated to be about 450 kb apart. We place *kan* between positions 250 and 330 and *nal* between 950 and 1050, giving a minimum separation of more than 600 kb. If the same relationship holds over the entire map of Michalka and Goodgal, the map should span about half of the *H. influenzae* Rd genome.

The map presented here will greatly enhance capabilities for both physical and genetic analyses of the *H. influenzae* genome. To further improve its physical resolution, we are completing the map of *Eag*I and *Nae*I fragments and hope to develop a set of mapped cosmid clones covering the entire genome. We are also mapping more cloned genes by Southern hybridization. Even with a detailed restriction map, genetic analysis in *H. influenzae* will still be limited by the small number of selectable markers known. To remedy this, we are preparing and mapping mini-Tn*10* insertions around the KW20 genome, using three different mini-Tn*10*s conferring resistance to kanamycin, tetracycline, and chloramphenicol, respectively (49). These will then provide many selectable markers distributed around the chromosome, which will be valuable tools for strain construction and genetic analysis.

The map is already providing unexpected information about strains in use. Strain BC200 was thought to be deleted for a defective prophage, but map analysis showed it to carry instead an inverted duplication of 45 kb. Strain BC200 was selected as a UV-resistant survivor after a high dose of UV (2), and its duplication may be similar to those seen in cryptic lysogens of *E. coli*, which arise when lambda lysogens are given high doses of UV (38). We do not know whether the putative prophage genome has been interrupted or deleted by this duplication or whether the lack of prophage expression results from undetectable changes elsewhere in the genome. Because the duplication is in inverted order, it will not readily be lost by recombination. BC200 has been the strain of choice for many studies of repair and recombination; at present, we have no reason to believe that the unsuspected presence of the duplication has affected any conclusions deriving from experiments with it.

ACKNOWLEDGMENTS

We thank G. Barcak for suggesting this project and C. Connelly, P. Hieter, J.-F. Tomb, and M. Chandler for advice. D. Valle was very generous with his OFAGE apparatus. P. Harriman performed the *hindIIIRM* gene Southern blot analysis. C. Squires, G. Barcak, G. Wilson, A. Wright, E. R. Moxon, D. McCarthy, R. Munson, and J. S. Kroll provided cloned genes, E. Hansen provided clinical isolates of *H. influenzae*, J. Scocca provided strain L-10, and J. Setlow provided strains MAP7 and BC200.

R.R. is supported by a postdoctoral fellowship from the Medical Research Council of Canada. The work was supported by a Public Health Service grant from the National Cancer Institute.

LITERATURE CITED

1. **Alexander, H. E., and G. Leidy.** 1951. Determination of inherited traits of *H. influenzae* by desoxyribonucleic acid fractions isolated from type-specific cells. J. Exp. Med. **93**:345–359.
1a. **Barcak, G. J., J.-F. Tomb, C. S. Laufer, and H. O. Smith.** 1989. Two *Haemophilus influenzae* Rd genes that complement the *recA*-like mutation *rec-1*. J. Bacteriol. **171**:2451–2457.
2. **Barnhart, B. J., and S. H. Cox.** 1968. Radiation-sensitive and radiation-resistant mutants of *Haemophilus influenzae*. J. Bacteriol. **96**:280–282.
3. **Barnhart, B. J., and S. H. Cox.** 1970. Recovery of *Haemophilus influenzae* from ultraviolet and X-ray damage. Photochem. Photobiol. **11**:147–162.
4. **Bautsch, W.** 1988. Rapid physical mapping of the *Mycoplasma mobile* genome by two-dimensional field inversion gel electrophoresis techniques. Nucleic Acids Res. **16**:11461–11467.
5. **Bayliss, H. A., and M. J. Bibb.** 1988. Organization of the ribosomal RNA genes in *Streptomyces coelicolor* A3(2). Mol. Gen. Genet. **211**:191–196.
6. **Berg, K. L., C. L. Squires, and C. Squires.** 1987. In vivo translation of a region within the *rrnB* 16S rRNA gene of *Escherichia coli*. J. Bacteriol. **169**:1691–1701.
7. **Brewer, B.** 1988. When polymerases collide: replication and the transcriptional organization of the *E. coli* chromosome. Cell **53**:679–686.
8. **Carle, G. F., and M. V. Olson.** 1984. Separation of chromosomal DNA molecules from yeast by orthogonal-field-alternation gel electrophoresis. Nucleic Acids Res. **12**:5647–5664.
9. **Catlin, B. W., J. W. Bendler, and S. H. Goodgal.** 1972. The type b capsulation locus of *Haemophilus influenzae*: map location and size. J. Gen. Microbiol. **70**:411–422.
10. **Chu, G., D. Volrath, and R. Davis.** 1986. Separation of large DNA molecules by contour-clamped homogeneous electric fields. Science **234**:1582–1585.

11. **Ellwood, M., and M. Nomura.** 1982. Chromosomal locations of the genes for rRNA in *Escherichia coli* K-12. J. Bacteriol. **149:**458–468.
12. **Ely, B., and C. J. Gerardot.** 1988. Use of pulsed-field-gradient gel electrophoresis to construct a physical map of the *Caulobacter crescentus* genome. Gene **68:**323–333.
13. **Feinberg, A. P., and B. Vogelstein.** 1984. Addendum. A technique for radiolabelling DNA restriction endonuclease fragments to high specific activity. Anal. Biochem. **137:**266–267.
14. **Feingold, J., Y. Bellofatto, L. Shapiro, and K. Amemiya.** 1985. Organization and nucleotide sequence analysis of an rRNA and tRNA cluster from *Caulobacter crescentus*. J. Bacteriol. **163:** 155–166.
15. **Fitzmaurice, W. P., and J. J. Scocca.** 1983. Restriction map and location of mutations on the genome of bacteriophage Hp1c1 of *Haemophilus influenzae* Rd. Gene **24:**29–35.
16. **Glaser, G., D. Amikam, and S. Razin.** 1984. Physical mapping of the ribosomal RNA genes of *Mycoplasma capricolum*. Nucleic Acids Res. **12:**2421–2426.
17. **Grundy, F. J., A. Plaut, and A. Wright.** 1987. *Haemophilus influenzae* immunoglobulin A1 protease genes: cloning by plasmid integration-excision, comparative analyses, and localization of secretion determinants. J. Bacteriol. **169:**4442–4450.
18. **Gulig, P. A., C. C. Patrick, L. Hermanstorfer, G. H. McCracken, and E. J. Hansen.** 1987. Conservation of epitopes in the oligosaccharide portion of the lipooligosaccharide of *Haemophilus influenzae* type b. Infect. Immun. **55:**513–520.
19. **Herriott, R. M.** 1971. Effects on DNA: transforming principle, p. 175–217. *In* A. Hollaender (ed.), Chemical mutagens: principles and methods for their detection, vol. 1. Plenum Publishing Corp., New York.
20. **Herriott, R. M., E. M. Meyer, and M. Vogt.** 1970. Defined nongrowth media for stage II development of competence in *Haemophilus influenzae*. J. Bacteriol. **101:**517–524.
21. **Hofman, J. D., R. H. Lau, and W. F. Doolittle.** 1979. The number, physical organization and transcription of ribosomal RNA cistrons in an archaebacterium: *Halobacterium halobium*. Nucleic Acids Res. **7:**1321–1333.
22. **Huysmans, E., and R. De Wachter.** 1986. Compilation of small ribosomal subunit RNA sequences. Nucleic Acids Res. **14:** r73–r118.
23. **Jarvis, E. D., R. Widom, G. LaFauci, Y. Setoguchi, I. Richter, and R. Rudner.** 1988. Chromosomal organization of rRNA operons in *Bacillus subtilis*. Genetics **120:**625–635.
24. **Keller, M., G. Burkhard, H. J. Bohnert, M. Mubumbila, K. Gordon, A. Steinmetz, D. Heiser, E. J. Crouse, and J. H. Weil.** 1980. Transfer RNA genes associated with the 16S and 23S rRNA genes of *Euglena* chloroplast DNA. Biochem. Biophys. Res. Commun. **95:**47–54.
25. **Koch, W., K. Edwards, and H. Kossel.** 1981. Sequencing of the 16S-23S spacer in a ribosomal RNA operon of *Zea mays* reveals two split tRNA genes. Cell **25:**203–213.
26. **Kohara, Y., K. Akiyama, and K. Isono.** 1987. The physical map of the whole *E. coli* chromosome: application of a new strategy for rapid analysis and sorting of a large genomic library. Cell **50:**495–508.
27. **Lee, J. J., and H. O. Smith.** 1988. Sizing of the *Haemophilus influenzae* Rd genome by pulsed-field agarose gel electrophoresis. J. Bacteriol. **170:**4402–4405.
28. **Lehner, A. F., S. Harvey, and C. W. Hill.** 1984. Mapping spacer identification of rRNA operons of *Salmonella typhimurium*. J. Bacteriol. **160:**682–686.
29. **Loughney, K., E. Lund, and J. E. Dahlberg.** 1982. tRNA genes are found between the 16S and 23S rRNA genes in *Bacillus subtilis*. Nucleic Acids Res. **10:**1607–1624.
30. **Lunnen, K. D., J. M. Barsomian, R. R. Camp, C. O. Card, S.-Z. Chen, R. Croft, M. C. Looney, M. M. Meda, L. S. Moran, D. O. Nwankwo, B. E. Slatko, E. M. Van Cott, and G. G. Wilson.** 1988. Cloning type II restriction and modification genes. Gene **74:** 25–32.
31. **Maniatis, T., E. F. Fritsch, and J. Sambrook.** 1982. Molecular cloning: a laboratory manual. Cold Spring Harbor Laboratory, Cold Spring Harbor, N.Y.
32. **McCarthy, D.** 1989. Cloning of the rec-2 locus of Haemophilus influenzae. Gene **75:**135–143.
33. **McCarthy, D., and S. S. Cox.** 1986. *rpe*, a *cis*-acting element from the *strA* region of the *Haemophilus influenzae* chromosome that makes plasmid establishment independent of recombination. J. Bacteriol. **168:**186–191.
34. **Michalka, J., and S. Goodgal.** 1969. Genetic and physical map of the chromosome of *Haemophilus influenzae*. J. Mol. Biol. **45:**407–421.
35. **Morgan, E. A., T. Ikemura, and M. Nomura.** 1977. Identification of spacer tRNA genes in individual ribosomal RNA transcription units of *Escherichia coli*. Proc. Natl. Acad. Sci. USA **74:**2710–2714.
36. **Munson, R., and S. Grass.** 1988. Purification, cloning, and sequence of outer membrane protein P1 of *Haemophilus influenzae* type b. Infect. Immun. **56:**2235–2242.
37. **Musser, J. M., J. S. Kroll, E. R. Moxon, and R. K. Selander.** 1988. Clonal population structure of encapsulated *Haemophilus influenzae*. Infect. Immun. **56:**1837–1845.
38. **Redfield, R. J., and A. M. Campbell.** 1987. Structure of cryptic lambda prophages. J. Mol. Biol. **198:**393–404.
39. **Riley, M., and S. Krawiec.** 1987. Genome organization, p. 967–981. *In* F. C. Neidhardt, J. L. Ingraham, K. B. Low, B. Magasanik, M. Schaechter, and H. E. Umbarger (ed.), *Escherichia coli* and *Salmonella typhimurium*: cellular and molecular biology, vol. 2. American Society for Microbiology, Washington, D.C.
40. **Roy, P. H., and H. O. Smith.** 1973. DNA methylases of *H. influenzae* Rd. J. Mol. Biol. **81:**427–444.
41. **Samiwala, E. B., V. P. Joshi, and N. K. Notani.** 1988. An estimate of the physical distance between two linked markers in *Haemophilus influenzae*. J. Biosci. **13:**223–228.
42. **Schwartz, D. C., and C. R. Cantor.** 1984. Separation of yeast chromosome-sized DNAs by pulsed-field gel electrophoresis. Cell **37:**67–75.
43. **Setlow, J. K., E. Cabrera-Juarez, and K. Griffin.** 1984. Mechanism of acquisition of chromosomal markers by plasmids in *Haemophilus influenzae*. J. Bacteriol. **160:**662–667.
44. **Smith, C. L., J. G. Econome, A. Schutt, S. Klco, and C. R. Cantor.** 1987. A physical map of the *Escherichia coli* K12 genome. Science **236:**1448–1453.
45. **Stuy, J.** 1985. Transfer of genetic information within a colony of *Haemophilus influenzae*. J. Bacteriol. **162:**1–4.
46. **Takaiwa, F., and M. Sugiura.** 1982. Nucleotide sequence of the 16S-23S spacer region in an rRNA gene cluster from tobacco chloroplast DNA. Nucleic Acids Res. **10:**2665–2676.
47. **Tomioka, N., K. Shinozaki, and M. Sugiura.** 1981. Molecular cloning and characterization of ribosomal RNA genes from a blue-green alga, *Anacystis nidulans*. Mol. Gen. Genet. **193:** 427–430.
48. **Waldman, A. S., W. P. Fitzmaurice, and J. J. Scocca.** 1986. Integration of the bacteriophage HP1c1 genome into the *Haemophilus influenzae* Rd chromosome in the lysogenic state. J. Bacteriol. **165:**297–300.
49. **Way, J. C., M. A. Davis, D. Morisato, D. E. Roberts, and N. Kleckner.** 1984. New Tn*10* derivatives for transposon mutagenesis and for construction of *lacZ* operon fusions by transposition. Gene **32:**369–379.
50. **Wenzel, R., and R. Herrmann.** 1988. Physical mapping of the *Mycoplasma pneumoniae* genome. Nucleic Acids Res. **16:** 8323–8336.